

Computational Fluid Dynamic Simulation of a Multiphase Fluid in Vertical Flow at High Reynolds Number

Iffat T. Shaikmohammad¹, Deep Bandyopadhyay¹, Karuna S. Koppula², André Bénard¹ and Charles A. Petty²,

¹Department of Chemical Engineering and Materials Science

²Department of Mechanical Engineering

Michigan State University

East Lansing, MI 48824-1105

Extended Abstract

Introduction

Gas-solids fluidization is a widely applied process in the petroleum, chemical, metallurgical and energy industries. Modeling of gas-solids fluidization processes provides an ancillary tool for minimizing the experimental efforts required for developing industrial plants. The purpose of this work is to evaluate the ability of a multiphase model to capture the flow physics associated with catalytic risers. In order to evaluate the effects of the suspended solids, simulations are performed for both single phase and multiphase flows (solids suspended in a gas). An Eulerian-Eulerian multiphase model is used that rely on the kinetic theory of granular flow for modeling the particle phase fluid properties, and various turbulence models are compared for the single-phase flow simulations.

The three-dimensional computational domain considered in all the simulations is shown in Fig. 1. Since the geometry considered is rectangular, a three dimensional Cartesian geometry is chosen with dimensions 0.17 x 1.20 x 0.19m, width (x) x height (y) x depth (z) respectively, in order to match with the experimental device (Ibsen et al., 2001). A staggered “hex-cooper” volume mesh was created using GAMBIT 2.2 with a very fine mesh near the walls and a rather coarse mesh at the center. The grid is made of 146,880 cells and 156,695 nodes (35, 37 and 121 nodes in x, y and z directions respectively). The steady state numerical simulations of a turbulent single-phase flow in

a channel were performed by considering air as a Newtonian fluid, with a Reynolds number of 10,000 based on hydraulic diameter.

For the geometry of the physical domain and the boundary conditions shown in Fig. 1, the following details are also needed. For single phase simulations, on the bottom side of the riser, an upward uniform velocity was specified; on the lower side, the pressure relative to a reference pressure was specified as zero. The simulation imposes a no slip condition at the wall. For two-phase simulations, in addition to the above conditions, the volume fraction of the dispersed phase on the inflow boundary was specified. The velocity of the primary phase and the velocity of the secondary phase were assumed equal and uniform. A zero backflow volume fraction was specified for the dispersed phase on the pressure patch. The initial conditions for single-phase simulations were that zero initial velocity was specified in the flow domain for all the single-phase simulations. The initial conditions for two-phase simulations were that the concentration of the secondary phase was zero in the flow domain for all the two-phase simulations.

Viscous Models in a Turbulent Duct Single-Phase Flow

The Reynolds Averaged Navier-Stokes (RANS-) equation and the Reynolds averaged continuity equation are used to compute the mean velocity and mean pressure fields. The Reynolds-averaged momentum equation is given by

$$\rho \left(u_j \frac{\partial u_i}{\partial x_j} \right) = -\frac{\partial p}{\partial x_i} + \frac{\partial}{\partial x_j} \left(\mu \frac{\partial u_i}{\partial x_j} \right) + \frac{\partial R_{ij}}{\partial x_j} + \rho \bar{g} \quad (1)$$

where $R_{ij} = -\rho \overline{u'_i u'_j}$ is the Reynolds stress. The various closure models vary on their approximation used for the Reynolds stress. “Eddy-Viscosity” models (introduced by Boussinesq, 1877) use a mathematical analogy to the stress-rate-of-strain relation for a Newtonian fluid. The Reynolds stress tensor is then modeled using an eddy (or turbulent) viscosity μ_t as

$$R_{ij} = -\rho \overline{u'_i u'_j} = \mu_t \left(\frac{\partial u_i}{\partial x_j} + \frac{\partial u_j}{\partial x_i} \right) - \frac{2}{3} \left(\rho k + \mu_t \frac{\partial u_i}{\partial x_i} \right) \delta_{ij} \quad (2.10)$$

On the other hand, the Reynolds Stress Model or RSM (Gibson et al., 1978); (Launder, 1989); (Launder et al., 1975) involves calculation of the individual Reynolds stress

components, $\overline{u'_i u'_j}$ using differential transport equations. The individual Reynolds stress components are then used to obtain closure of the Reynolds-averaged momentum equation

Realizability Diagram for Single Phase Channel Flow

Single-phase flow simulations were performed with Fluent using the Spalart-Allmaras (Spalart et al, 1992), the Standard $k-\omega$ (Wilcox, 1998), the Realizable $k-\varepsilon$ (Shih et al., 1995) and the Reynolds Stress Model (Gibson et al., 1978; Launder, 1989; Launder et al., 1975) for the geometry shown in Fig. 1. To assess the realizability of the various viscous models used, the eigenvalues of the Reynolds stress were computed for each of these models. An algebraic property of the Reynolds stress is that its eigenvalues must be positive. The invariants of the Reynolds stress can be plotted using a “realizability or Lumley diagram” as shown in Figs 2 and 3 at a specified height for several points across the channel.

It was found that all the viscous models proved to be realizable except for the Spalart-Allmaras. The Spalart-Allmaras is found to be highly unrealizable for this problem. In addition, the Standard $k-\omega$ model and Realizable $k-\varepsilon$ model, which use the Boussinesq hypothesis, predicts that invariant III of the anisotropic tensor \underline{b} associated with the Reynolds stress (see Fig. 2) is almost zero. This is due to the mathematical construction of the eddy viscosity model and the nature of the flow (it is simple to derive the eigenvalues and observe that $\text{III}=0$ for models based on the Boussinesq approximation).

Gas-Solid Simulations

The conservation equations for the solid phases are based on the kinetic theory for granular flow and are not provided here for brevity. The theory of the multiphase model is based on kinetic theory of non-uniform gasses, as presented by Chapman et al. (1970). The model was developed and matured through various publications such as Jenkins et al. (1983), Lun et al. (1984), Jenkins et al. (1987), Gidaspow et al. (1992) and Gidaspow (1994). The gas phase calculations are done using a continuum approach based on a

three-dimensional Eulerian realizable $k - \varepsilon$ multiphase model. A two-phase realizable eddy viscosity model for the Reynolds stress is used in this work as a closure for the RANS-equation. All the simulations were performed using a segregated solver. The upwind scheme is used in all the numerical simulations obtained with Fluent. The set of algebraic equation is solved using the Algebraic Multigrid Method (Hutchinson et al., 1986). The coupling is achieved through the pressure and interphase exchange coefficients using the Phase Coupled SIMPLE algorithm for the pressure-velocity coupling, (Patankar, 1980).

Experimental set up of the 1/9 scale Cold Circulating Fluidized Bed Boiler

The dimensions of the experimental set up of Ibsen et al. (2001), used to validate the simulations, were 1.5 m x 0.19 m x 0.17 m corresponding to Height(x) x Depth(y) x width (z) respectively. The entrance of the cyclone was located at the rear of the riser, 1.2 m above the primary air distributor. No secondary air was used. A cyclone was used to separate the solids, which passed a particle seal designed as a bubbling bed, before being reintroduced in the lower part of the riser. The amount of solids recirculated was adjusted to give a pressure drop across the riser equal to 2.7 kPa (corresponding to 8KPa in the full-scale boiler). A detailed description of the model is given elsewhere (Johnsson et al., 1999).

Parameters for the gas-solid simulations

The flow parameters applied in the gas-solid simulations are tabulated in Table 1. A uniform plug flow is assumed for the gas phase at the inlet with a superficial velocity of 1.0 m/s (Reynolds number=12,156). The inlet flux of the solid phase is assumed to be equal to the outlet flux. No-slip boundary conditions are adopted along the walls for all phases. As initial conditions, the solid phases are evenly distributed in the lower half of the riser with zero velocity. Considering however the larger number of cells required in three dimensions, the simulations were terminated after 20 s real time and the averaged results were obtained which was found to be adequate. The mean volume length diameter is used for the solid phase (Peirano et al., 2000), which is $d_p = 45 \mu\text{m}$. The amount of solids in the numerical model was 9 kg. This was a result of adjusting the amount of

solids in the riser to give a pressure drop over the riser height comparable to the experiment.

Simulation time

Simulations of fluidized beds with about 9 kg of solids took about 8 days to simulate 20 seconds of real time. The simulations were run on a 6-node computer with a 2.2 GHz processor. In comparison (Zhang et al., 2001) used 101 days to simulate 21 s with their fine grid on a SGI Origin 200.

Numerical results and discussions

The particle velocities at various profiles (an example is shown in Fig. 4), were not found to be in good agreement with the experimental findings. The experimental findings indicate a constant decrease in the axial and span wise velocities at the centerline whereas in the numerical model this trend for the particle velocities was not captured. Also, the predicted solid velocities near the wall deviate much from the experimental findings which are an indication that wall boundary conditions for the solid particles is quite complex.

The realizability plot for the $\overline{u'u'}$ associated with the primary phase computed with the Realizable $k - \varepsilon$ is shown in Fig. 5. In the two-phase simulations of gas-solid flows, the realizable $k - \varepsilon$ model proves to be highly unrealizable for the secondary phase (solid) at and near the centerline while it is realizable near the walls.

Summary and Conclusions

The objective of this work was to assess the performance of single-phase flow and two-phase turbulent flow models implemented in FLUENT 6.2 using experimental data and the realizability diagram for the Reynolds stress. The Reynolds stress must have positive or zero eigenvalues to be physical and the invariant diagram bounds the region corresponding such eigenvalues.

The various turbulence models applied in the single phase flow simulations proved to be realizable except for the Spalart-Allmaras model (Spalart et al., 1992) which showed to be unrealizable at various locations. Moreover, the Realizable $k - \varepsilon$ model (Shih

et al., 1995), which was realizable for single-phase flows, became unrealizable for the primary phase in the two-phase flow simulations. It is unclear if the inaccuracies arise due to the numerical implementation or the coupling of the granular model with the turbulence model. In addition, the gas-solid flow model was not able to predict the right order of pressure drop across the riser. Also, the predicted time averaged profiles of the axial and span wise particle velocities showed poor agreement with the experimental findings (Ibsen et al., 2001). The gas-solid flow numerical model does not appear to be capable of predicting the correct interaction of the turbulent gas phase and particles. It was observed that the dispersion of the secondary phase is under predicted and the numerical results did not predict a dense bottom bed as seen in the experimental set-up.

Acknowledgements

This work was funded by the Center for Multiphase Transport Phenomena (NSF I/UCRC-MTP, NSF/ECC 0331977). The support of the Fluent and other center members is gratefully acknowledged.

References

- Boussinesq, J., 1877, "Essai sur la théories des eaux courantes," Mémoires présentés par divers savants a l'Académie des Sciences de l'Institut National de France, 23(1).
- Chapman S., and Cowling T. G., 1970, "The Mathematical Theory of Non-Uniform Gases", 3 ed. Cambridge University Press.
- Fluent 6.2, User's Guide, Fluent Incorporated, Lebanon, NH.
- Gibson M. M. and Launder B. E., 1978, "Ground Effects on Pressure Fluctuations in the Atmospheric Boundary Layer", J. Fluid Mech., 86:491-511.
- Gidaspow D., 1994, "Multiphase Flow and Fluidization", Academic Press, Inc., U.K.
- Gidaspow D., Bezburuah R., and Ding J., 1992, "Hydrodynamics of circulating fluidized beds: Kinetic theory approach", In: Fluidization VII (O. E. Potter, Ed.). Engineering Foundation. New York. pp. 75–82.
- Hutchinson B. R. and Raithby G. D., 1986, "A Multigrid Method Based on the Additive Correction Strategy, Numerical Heat Transfer", 9:511-537.
- Ibsen C.H., Solberg T. and Hjertager B.H., 2001, "Evaluation of a Three-Dimensional Numerical Model of a Scaled Circulating Fluidized Bed", Industrial & Engineering Chemistry Research, Vol. 40, no. 23, pp. 5081-5086.
- Ibsen C.H., Hjertager B.H., Solberg T. and Johnsson F., 2001, "Laser Doppler Anemometry Measurements in a Circulating Fluidized Bed of Metal Particles",

- ICMF-2001, 4th International Conference on Multiphase Flow, May 27 - June 1 2001, New Orleans, Louisiana, USA.
- Jenkins J. T. and Mancini F., 1987, “Balance laws and constitutive relations for plane flows of a dense mixture of smooth, nearly elastic, circular disks”, *J. App. Mech.* 54, 27–34.
 - Jenkins, J. T. and Savage S. B., 1983, “A theory for the rapid flow of identical, smooth, nearly elastic, spherical particles”, *J. Fluid Mech.* 130, 187–202.
 - Johnsson F., Vragar A. and Leckner B., 1999, “Solids flow pattern in the exit region of a CFB-furnace-influence of exit geometry”, 15th Int. Conf. on Fluidised Bed combustion, Savannah.
 - Launder B. E., 1989, “Second-Moment Closure: Present and Future”, *Inter. J. Heat Fluid Flow*, 10(4):282-300.
 - Launder B. E., Reece G. J., and Rodi W., 1975, “Progress in the Development of a Reynolds-Stress Turbulence Closure”, *J. Fluid Mech.*, 68(3):537-566.
 - Lun et al, Lun C. K. K., Savage S. B., Jeffrey D. J. and Chepurniy N., 1984, “Kinetic Theories for Granular Flow: Inelastic Particles in Couette Flow and Slightly Inelastic Particles in a General Flow Field”, *J. Fluid Mech.*, 140:223-256.
 - Patankar S. V., 1980, “Numerical Heat Transfer and Fluid Flow”, Hemisphere, Washington D.C.
 - Peirano E., Leckner, B., 2000, “A mean diameter for numerical computations of polydispersed gas-solid suspensions in fluidization”, *Chem. Eng. Sci.* 55. 1189-1192.
 - Shih et al., 1995, “A New $k - \varepsilon$ Eddy-Viscosity Model for High Reynolds Number Turbulent Flows - Model Development and Validation”, *Computers Fluids*, 24(3):227-238.
 - Spalart P. and Allmaras S. 1992, “A one-equation turbulence model for aerodynamic flows”, Technical Report AIAA-92-0439, American Institute of Aeronautics and Astronautics.
 - Wilcox D. C., 1998, “Turbulence Modeling for CFD”, DCW Industries, Inc., La Canada, California.
 - Zhang D. Z., VanderHeyden W. B., 2001, “High-resolution three-dimensional numerical simulation of a circulating fluidized bed”, *Powder Technology.* 116. 133-141.

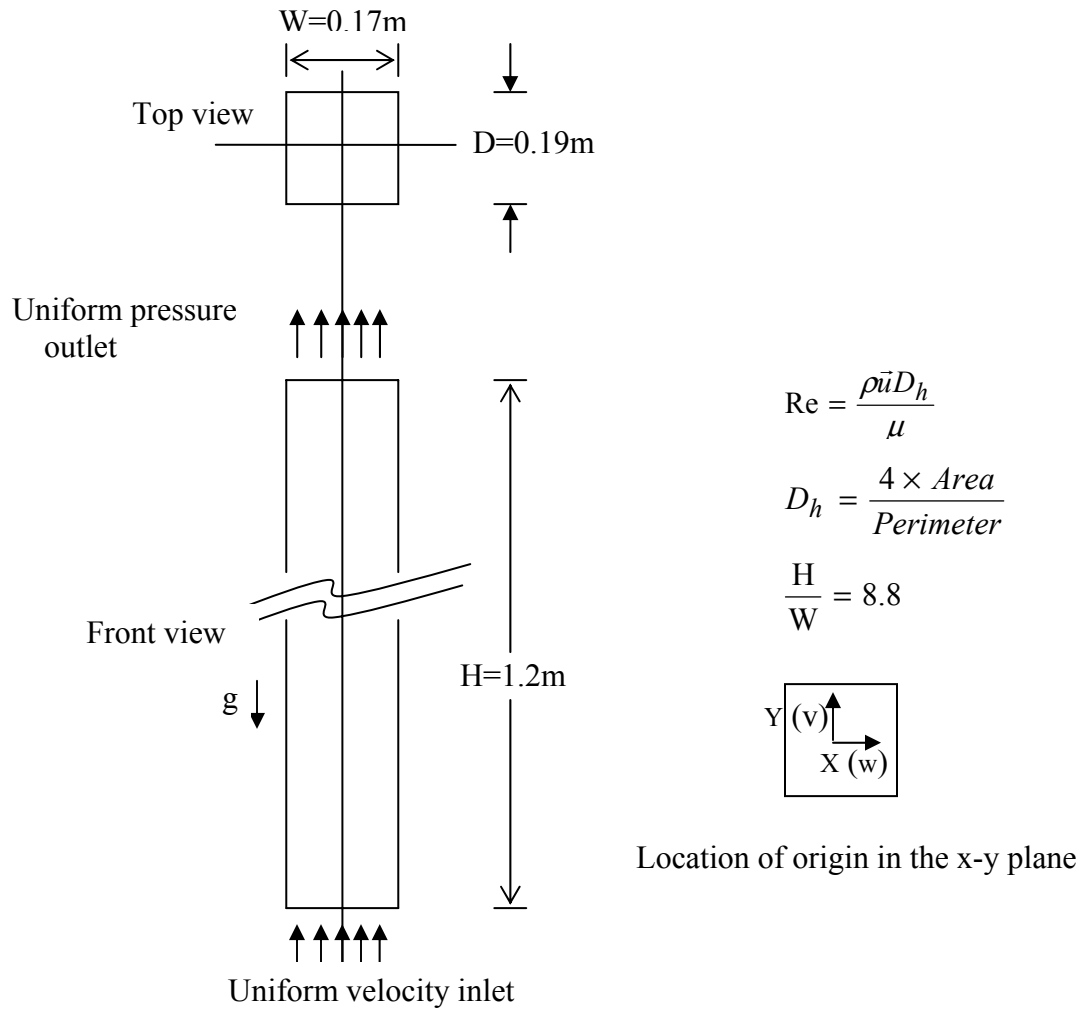


Figure1: Geometry of 3D-vertical upward channel flow considered in the simulations.

Table 1: Parameters for the fluid-solid simulations

Dimensions of the geometry ($H \times W \times D$)	$X \times Y \times Z$	1.2 x 0.17 x 0.19
Number of Mesh Cells	N_{cell}	146,880
Gas Density	ρ_g	1.2 kg/m ³
Gas Velocity	V_g	1.0 m/s
Gas Viscosity	μ_g	1.8 E-05 kg/ms
Particle diameter	d_p	45 μ m
Particle Density	ρ_p	7800 kg/m ³
Amount of Solids Used	m_s	9 kg
Volume fraction of solid	α_s	0.03572
Restitution coefficient	e	0.95
Maximum Solid Packing	$e_{s,max}$	0.64

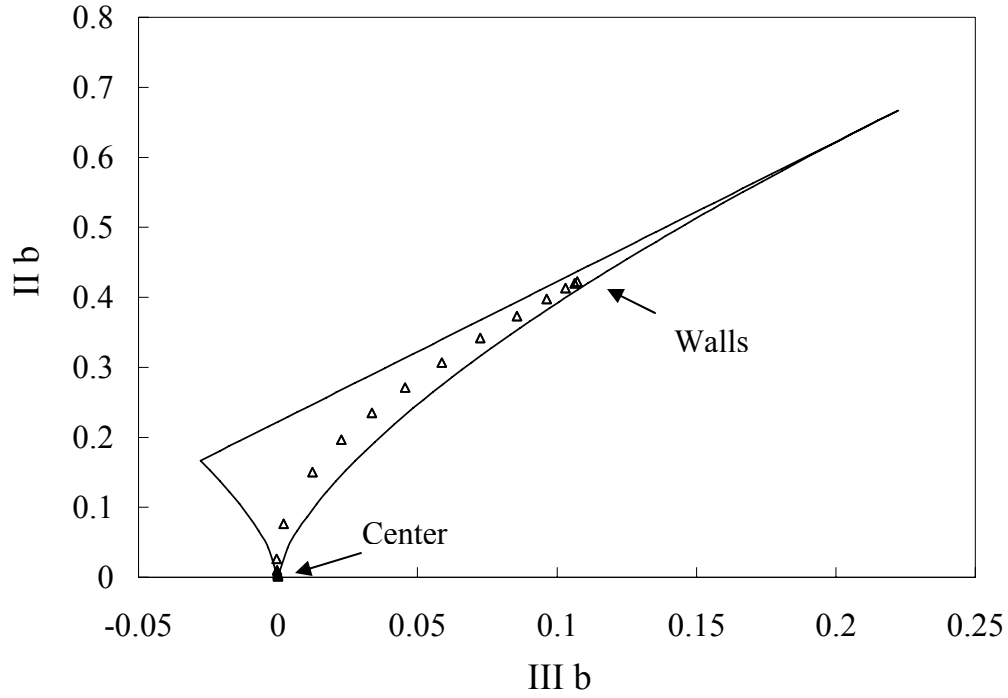


Figure 2. Realizability plot for the Reynolds stress model where $\underline{\underline{b}} \equiv \frac{\overline{\underline{u}'\underline{u}'}}{\text{tr}(\overline{\underline{u}'\underline{u}'})} - \frac{1}{3}\underline{\underline{\delta}}$, $II_b \equiv \text{tr}(\underline{\underline{b}} \cdot \underline{\underline{b}})$, $III_b \equiv \text{tr}(\underline{\underline{b}} \cdot \underline{\underline{b}} \cdot \underline{\underline{b}})$. The computed eigenvalues from the numerical solution must be within the outlined domain to have positive eigenvalues. The solutions were obtained for $Y/D=0$ and $Z/H=-0.5$ for points across the center of the channel.

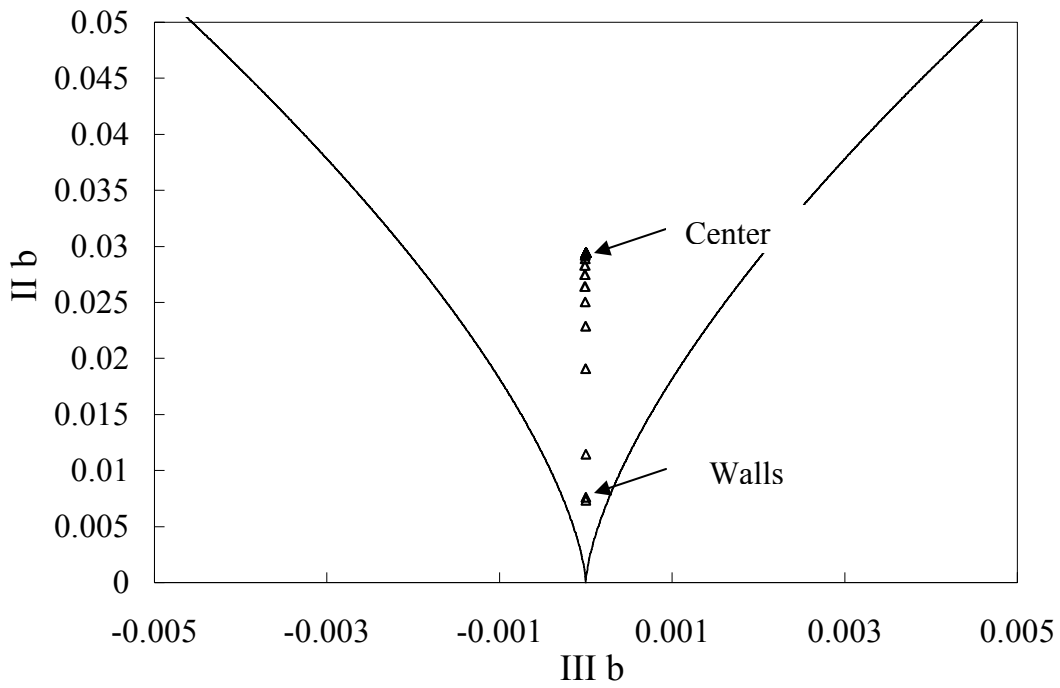


Figure 3. Realizability plot for the Realizable $k-\varepsilon$ model at $Y/D=0.48$ $Z/H=-0.5$ for points crossing the channel.

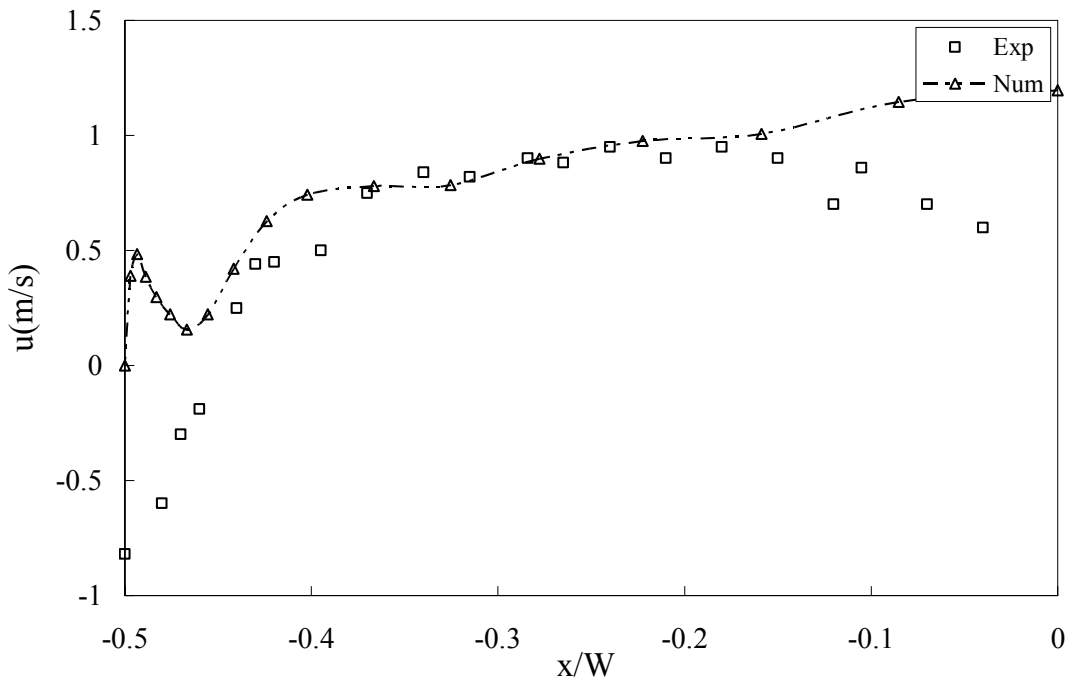


Figure 4. Plot of comparison between the measured (Ibsen et al., 2001) and computed axial particle velocities at profile 2. ($x = 0$ is the center of the channel).

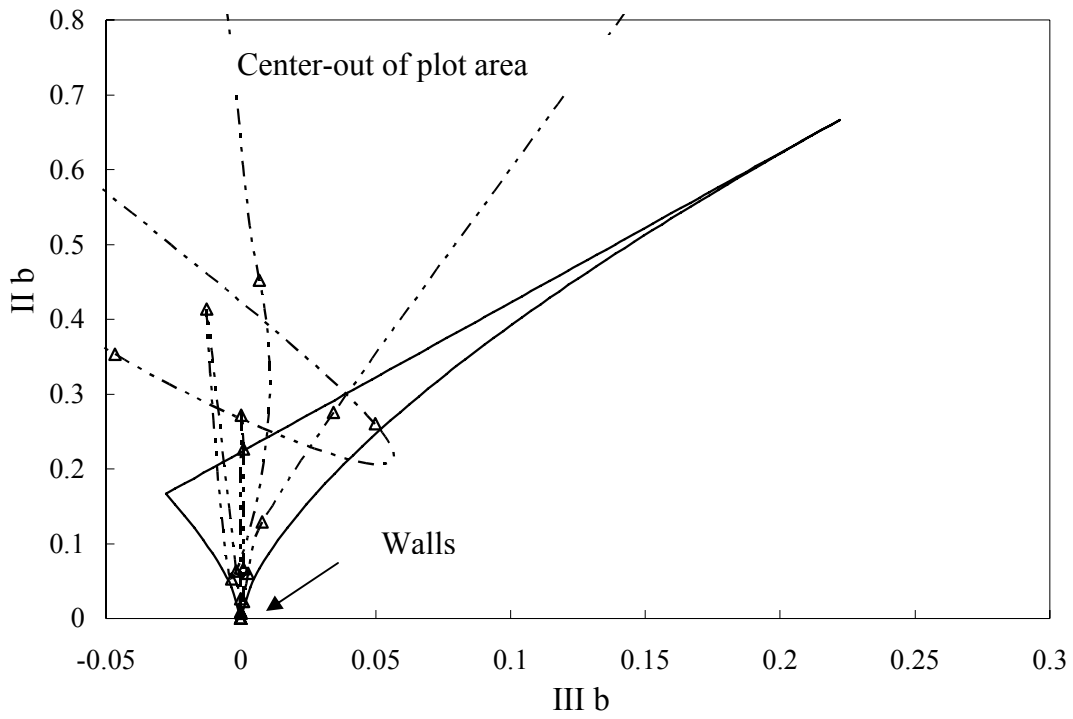


Figure 5. Realizability plot for $\overline{u'u'}$ associated with the primary phase computed with the Realizable $k - \varepsilon$ at $Z/H = -0.4$ and $Y/D = 0$.